Nanostructured CdS prepared on porous silicon substrate: Structure, electronic, and optical properties

P. Zhang, P. S. Kim, and T. K. Sham

Citation: Journal of Applied Physics **91**, 6038 (2002); doi: 10.1063/1.1461888
View online: http://dx.doi.org/10.1063/1.1461888
View Table of Contents: http://scitation.aip.org/content/aip/journal/jap/91/9?ver=pdfcov
Published by the AIP Publishing

Nanostructured CdS prepared on porous silicon substrate: Structure, electronic, and optical properties

P. Zhang, P. S. Kim, and T. K. Sham
Department of Chemistry, The University of Western Ontario, London, Ontario N6A 5B7, Canada

(Received 6 August 2001; accepted for publication 28 January 2002)

Nanostructured CdS was deposited electrochemically on porous silicon (PS) substrate/cathode. The PS-supported CdS deposits were found to be uniformly packed particles of ~100 nm, each of which is an aggregate of smaller clusters of several nanometers as revealed by scanning electron microscope and confirmed by glancing incidence x-ray powder diffraction. No significant CdS deposition into the pore of porous silicon is found under the reported experimental conditions. X-ray absorption fine structures (XAFS), both extended x-ray absorption fine structure and x-ray absorption near edge structures, across the S and the Si *K* edge of the samples have been investigated. The structure and electronic properties of the CdS/PS composite are discussed on the basis of the XAFS results obtained using multichannel detection (total electron and x-ray fluorescence yields) from a series of CdS and PS samples. The optical luminescence behavior of CdS/PS was also investigated utilizing a technique often referred to as synchrotron x-ray excited optical luminescence (XEOL). By selecting excitation photon energies near the Si and the S *K* edge, the luminescence originated from both CdS and PS can be distinguished in the XEOL spectra.
 [DOI: 10.1063/1.1461888]

I. INTRODUCTION

In recent years, the study of nanometer-scale materials (usually 1–100 nm, also called nanomaterials) generates intense interest because at this scale materials exhibit many properties that cannot be found in their bulk counterparts.[1,2] Generally for many practical purposes, nanomaterials should be assembled on a suitable substrate and it is desirable in many cases that the nanoassembly and the supporting substrate are both functional. For example, many research works[3] have been dedicated to the fabrication of various patterned nanomaterials on silicon substrate, the most important materials in modern electronic industry, so that functions brought by the nanomaterials can be applied to the Si-based electronic devices.

Porous silicon (PS) is a nanostructured silicon material prepared by electrochemically etching a silicon wafer in a HF solution.[4] The observation of intense luminescence from PS at room temperature[4] makes it very promising to integrate the very well-established silicon technology to the field of optoelectronic system where the indirect-band gap bulk Si materials can now find applications. Furthermore, PS was also found to be a more efficient substrate than plain Si wafer on which high quality carbon nanotube assembly with excellent device performance can be fabricated.[5] It has also been shown that such a PS-based nanofabrication technique can be employed to form many metallic nanostructures on PS such as Pd,[6] Cu,[7] Au,[8,9] Pt,[9] Ag,[10] Rh,[11] and very recently some semiconductors such as CdS.[12,13] In this article, we report a systematic study on the morphology, structure, electronic, and optical properties of the CdS/PS nanocomposites.

II. EXPERIMENT

PS samples were formed utilizing a single-cell electroplating configuration with the silicon wafer as the anode and a Pt foil as the counter electrode. Regular N-doped $n-$ silicon wafer was electrochemically etched in 25% HF/ethanol solution at a 50 mA/cm^2 constant current. The as-prepared PS electrode was immediately rinsed with alcohol, acetone, and dimethylsulfoxide (DMSO) and then acts as a cathode in the same cell for the next CdS deposition. The method for preparing CdS on PS substrate is similar to that reported by Baranski *et al.*[14] Briefly, in the DMSO solution of 10 g/L $CdCl_2$ and 6 g/L S solution, a small constant current was kept between the PS cathode and Pt foil counter electrode at the temperature of 110–120 °C. Under such a carefully controlled condition, the S will gain electrons from cathode to become S^{2-} slowly and then react with Cd^{2+} to form CdS on the surface of PS cathode.[13] The procedure is illustrated in Fig. 1. After CdS deposition, the sample was rinsed with hot DMSO, acetone, and ethanol in sequence to remove the unreacted S and Cd^{2+} species.

The morphology of the CdS/PS composite was studied using a Topometrix TMX 2000 Explorer atomic force microscope with tapping mode and a Hitachi S-4500 field-emission scanning electron microscope (SEM) performed at Surface Science Western (SSW). X-ray powder diffraction results were collected at a glancing angle ($\theta \sim 2°$) with an INEL x-ray powder diffractometer using a Cu $K\alpha$ source. The diffractometer is equipped with a CPS-120 curved detector to collect x rays spanning 120° two-theta simultaneously.

The synchrotron radiation study was conducted at the double crystal monochromator (DCM) beam line of the Canadian Synchrotron Radiation Facility (CSRF) at the Synchrotron Radiation Center (SRC), University of Wisconsin-Madison. In the x-ray near edge structure (XANES) study, total electron yield (TEY) and x-ray fluorescence yield (FLY) were recorded simultaneously using specimen current

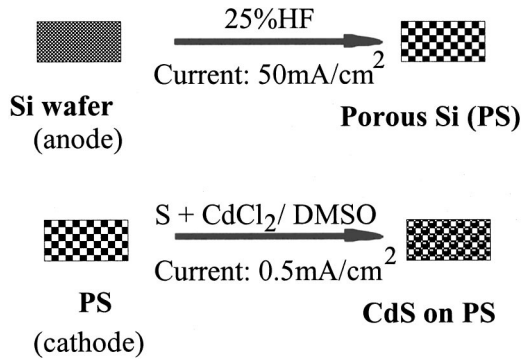

FIG. 1. Schematic of preparation of CdS/PS using an electrochemical method.

and a multichannel-plates detector, respectively. TEY and FLY probe the surface/near surface and the bulk of the specimen, respectively. Synchrotron x-ray excited optical luminescence (XEOL) was detected using a JY H-100 monochromator that is equipped with a Hamamatsu 943-02 photomultiplier. The XEOL technique involves the measurement of the photoluminescence at selected excitation photon energies from a synchrotron radiation light source.

III. MORPHOLOGY OF CdS DEPOSITS ON PS

Figure 2 shows the scanning electron microscope images of plain PS, Fig. 2(a) and CdS/PS, Figs. 2(b), and 2(c). The micrograph of plain PS in Fig. 2(a) shows a porous structure, each pore being ~600 nm in diameter. This kind of macroporous morphology is typical for *n*-type PS due to the nature of the doping.[8] Figure 2(b) reveals that the cathodic deposition results in CdS particles in the order of ~100 nm uniformly distributed on the PS surface. We also conducted cross-section SEM investigation (not shown here) on the CdS/PS sample but found no evidence for the formation of significant CdS deposits inside the PS pores. Figure 2(c) shows the high-magnification SEM images of the CdS/PS sample. Interestingly, we observed that the ~100 nm CdS particles are made up of smaller nanocrystallites, each of which is several nanometers. The PS surface in the high-magnification SEM image also shows very small pores (micropores) with comparable size to the CdS clusters, which is consistent with the model about the formation of *n*-type macropores,[8] i.e., that the macropores are formed through collapsing of the micropores during the electroetching and rinsing process. Actually, it is the Si nanostructure within the microporous but not the macroporous structure that are responsible for the so-called ''quantum-confinement-induced luminescence'' of PS.[15] At present, the growth mechanism of the observed CdS nanostructure is not very clearly understood. We attribute the growth to a PS-nanotemplate-assisted formation of CdS nanostructure since such nanostructures are not observed in the CdS-electrodeposition on a plain Si wafer under similar conditions.[16] More details concerning the CdS growth mechanism must await further kinetics and *in situ* studies of the electrodeposition and will be reported elsewhere. Here, however, we remain focused on the study of the properties of CdS/PS.

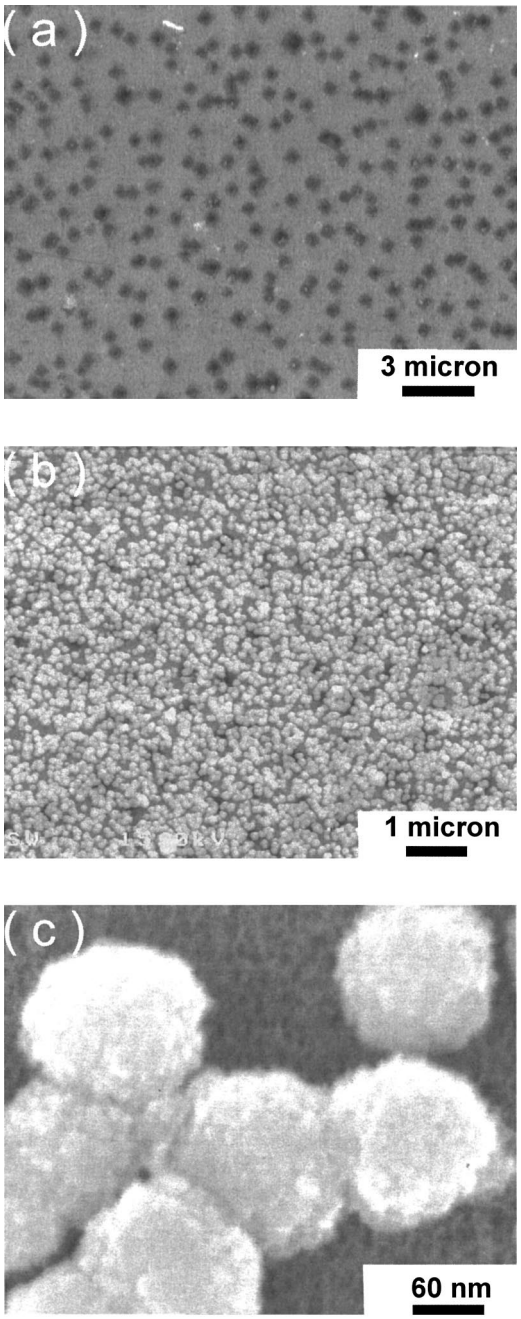

FIG. 2. SEM images of plain (a) PS and (b),(c) CdS/PS.

IV. STRUCTURE AND ELECTRONIC PROPERTY STUDIED BY X-RAY METHODS

A. Glancing incidence x-ray diffraction

The structure of the CdS nanoclusters revealed in SEM can be confirmed by the x-ray diffraction (XRD) study. Figure 3 shows the glancing incidence XRD patterns of CdS/PS, plain PS and CdS/PS–PS (meaning that the PS background was subtracted from CdS/PS). As is well known, when the size of microcrystallite becomes small enough, the diffraction peak will exhibit a size dependent broadening. The average size of CdS clusters can be estimated using the Scherrer equation[17]

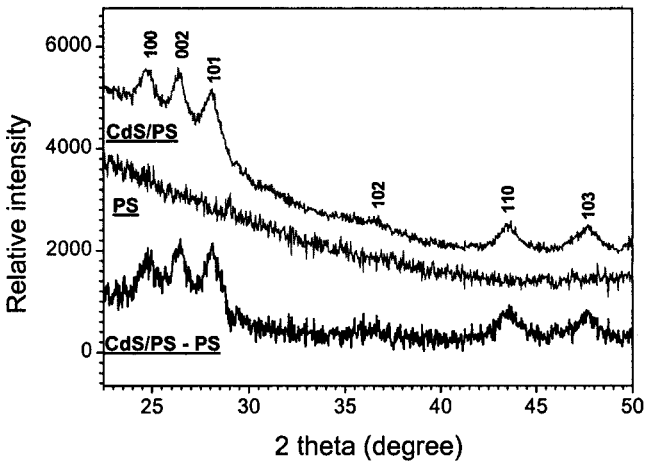

FIG. 3. Glancing incidence x-ray diffraction patterns of CdS/PS sample (before subtracting PS background), plain PS and CdS/PS–PS (after subtracting the PS background from the composite).

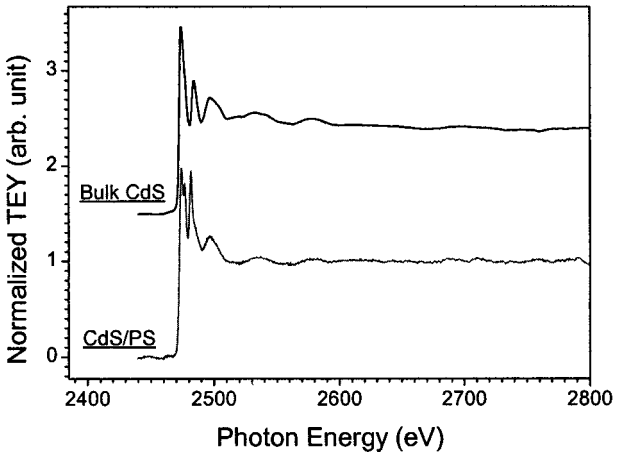

FIG. 4. S *K*-edge XAFS spectra of CdS/PS and bulk CdS collected in the TEY mode.

$$\tau = K\lambda/\beta_\tau \cos\theta, \tag{1}$$

where K is the shape factor of a value of 0.9, λ is the wavelength of the incident x ray, and β_τ is given by $(B^2 - b^2)$ in radian units where B is the width at half maximum of the diffraction peak and b is the diffraction peak width of corresponding bulk materials. When the (110) diffraction peak at 43.6° in Fig. 2 is chosen for the calculation, we obtain an average crystallite size of ~6 nm.

From the XRD results, one can further gain information about the crystal structure of the CdS deposits. The relative diffraction peak intensity and corresponding *d* spacing of the CdS clusters as well as those of standard CdS[18] are listed in Table I. From the data, we found that our CdS deposits are consistent with a Greenockite hexagonal crystalline structure.

B. X-ray absorption near edge structure

X-ray absorption fine structure (XAFS) explores variations in the absorption coefficient of matter as a function of photon energy above an absorption threshold. Very rich information about the local structural and electronic properties of materials can be gained using this technique.[19] It is particularly suited to the study of various nanosystem since the XAFS probes mainly short-range order surrounding the absorbing atom. Figure 4 shows the S *K*-edge XAFS spectra of both CdS/PS and bulk CdS samples. It is convenient to divide the XAFS into two regions, i.e., XANES region ranging from ~20 eV below the edge threshold to ~40 eV above the threshold and extended XAFS region which is the next several hundred electron volts above the XANES. We will first discuss the results in the near edge range.

Figure 5 shows the S *K*-edge XANES spectra in TEY of the CdS/PS sample and the bulk CdS. In the XANES of CdS, a peak at the threshold, often referred to as a whiteline, occurs at the absorption edge jump (~2472 eV) followed by a few less intense resonances in the higher energy region. The whiteline arises from a dipole transition from the S 1 s to the *p* densities of states in the conduction band. Comparing with bulk CdS, some features appear in the spectrum of the nano-CdS. First, the threshold (the point of inflection of the rising edge) and the whiteline of the nano-CdS shift lightly to higher energy (0.4–0.5 eV) relative to bulk CdS (see the inset first derivative spectra), indicating a wider band gap in the nanostructure than in the bulk. Second, XANES features were found at ~2477 and ~2482 eV in the CdS/PS sample. Comparing with the $CaSO_4$ reference shown in the same figure, we can attribute the peak at ~2482 eV to the reso-

TABLE I. XRD data of CdS/PS sample and standard CdS reference.

CdS on PS[a]		Greenockite[b]		
d spacing/Å	Relat. int.	*d* spacing/Å	Relat. int.	*hkl*
3.595	79.5	3.586	62	100
3.366	100	3.360	91	002
3.166	96.4	3.163	100	101
2.444	28.7	2.452	29	102
2.074	39.7	2.070	48	110
1.904	38.5	1.900	50	103

[a]Data obtained in Fig. 2 (from CdS/PS–PS).
[b]Data from Ref. 16.

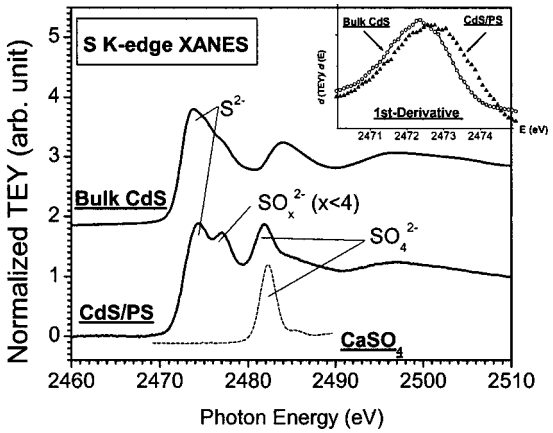

FIG. 5. S *K*-edge XANES spectra of CdS/PS, bulk CdS and $CaSO_4$ references measured in the TEY mode. The inset is the first derivative spectra of CdS/PS and bulk CdS, respectively.

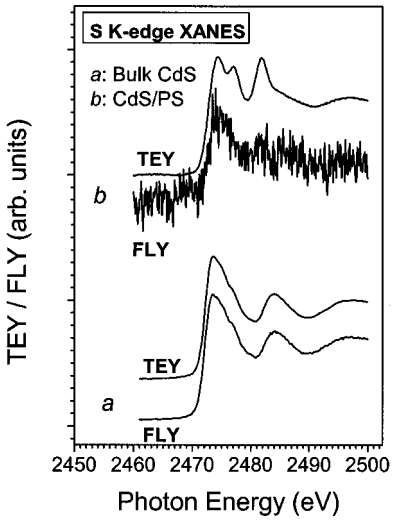

FIG. 6. S *K*-edge XANES of CdS/PS and bulk CdS collected in multichannel detection modes—TEY and FLY.

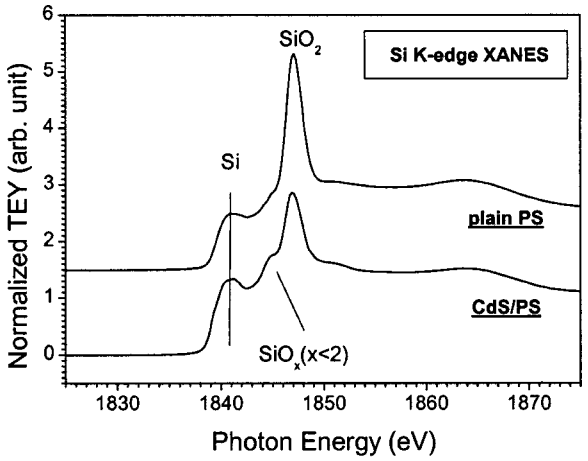

FIG. 7. Si *K*-edge XANES (in TEY) of CdS/PS and plain PS prepared under similar conditions.

nance of SO_4^{2-}. The feature at ~2477 eV are most likely from SO_3^{2-}-like species. A similar feature from SO_3^{2-} has been reported in the literature.[20]

The location of the oxide species in the CdS deposits is interesting because it can help us to understand the structure and properties of the CdS deposits. As noted earlier, we conducted a multichannel XANES study for the nano-CdS and the bulk, i.e., TEY and FLY spectra were collected simultaneously. Since the probing depths for TEY and FLY associated with photoexcitation at these energies are around several and hundreds of nanometers, respectively (x-ray fluorescence photons have a much larger attenuation length than that of electrons resulting from the excitation),[21,22] it is thus established that the TEY spectrum is more surface sensitive whereas FLY more bulk sensitive. In Fig. 6, the TEY and FLY spectra of the bulk [curve (a)] and nanostructured CdS [curve (b)] are given. One can see that the bulk CdS displays identical XANES in TEY and FLY spectra whereas the nano-CdS does not. That is, that the strong resonances at ~2477 and ~2482 eV of nano-CdS in the TEY spectra are considerably reduced in FLY. Based on the difference of the probing depth of the two yields, it is thus plausible that the oxide components are mostly located on the surface of CdS aggregate. If the oxide-related resonance in the TEY spectra were from the surface/interface/grain boundary of each CdS cluster (grain) that form the larger aggregate, it would have been detected in the FLY also. A possible reason is that the CdS clusters in the core of the aggregates are much less susceptible to oxidation, giving little contribution to the oxide-related resonance in FLY spectrum. Another less likely but possible origin of the oxide is related to the oxidation of the unreacted S, since sequential rinse of CdS/PS after preparation with DMSO, acetone, and alcohol may not be able to remove all the unreacted S. In fact, in a recent study of CdS aggregates of dendrimer-protected clusters of ~2 nm, similar observation was made.[22] Further analysis is required to reach a more satisfactory conclusion.

The Si *K*-edge XANES was also measured to study the effect of CdS deposition on the PS substrate. Figure 7 shows the TEY–XANES spectra of both CdS/PS and plain PS measured after the samples were stored in the ambient atmosphere for about 1 week. After the one-weak exposure in the air, both samples display a peak at ~1847 eV which is a well-known feature of Si–O bonding in silicon dioxide. The most noticeable difference between the two XANES spectra is that the SiO_2 resonance in the plain PS is very intense and sharp. Comparatively, this feature in the CdS-covered PS sample is broader and the intensity is considerably suppressed. A closer examination reveals a noticeable feature at ~1844 eV existing in the XANES of CdS/PS sample. This feature is believed to relate to suboxide species.[23] The earlier observations indicate that CdS deposition inhibits to some extent the oxidation of the PS substrate, which is not observed in the case of electroless deposition of metal on PS, in which the oxidation of PS is enhanced and the formation of suboxide is clearly noticeable.[8] Further, it suggests that the interaction between the PS substrate and the CdS deposits are strong enough to prevent the PS from further oxidation. However, since the CdS deposits do not cover all the surface area of the PS, the PS substrate still undergoes some oxidation.

C. Extended x-ray absorption fine structure

Figure 8 shows the *k*-space S *K*-edge extended x-ray absorption fine structure (EXAFS) spectra of both the bulk and the nanosample. The spectra are truncated at ~8.3 $Å^{-1}$ to leave out contribution from Cl^{-1} impurity (from the starting material).[24] The similarity of the EXAFS wiggles between the two spectra is obvious. This result indicates that the CdS deposits have identical crystallite structure with the bulk counterpart (hexagonal), which is in good accord with our XRD analysis. The Fourier transform (FT) analysis of EXAFS shows that the first shell bond distance is the same in both systems with some disorder although the data length is not sufficient for a detailed quantitative analysis.

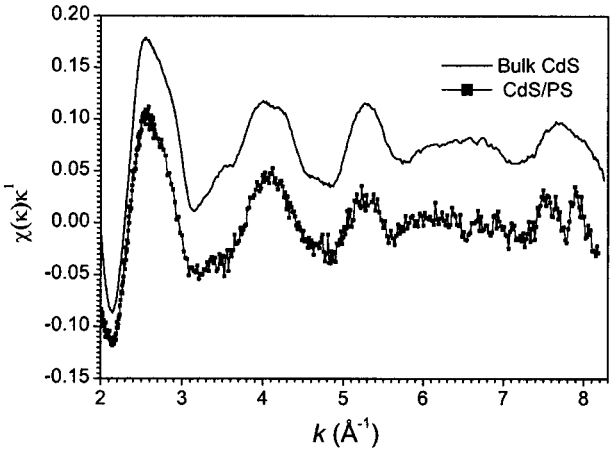

FIG. 8. (a) *k*-space EXAFS and (b) FT-transformed EXAFS of CdS/PS and bulk CdS around the S *K* edge.

V. ORIGIN OF LUMINESCENCE OF CdS/PS COMPOSITE INDUCED BY SYNCHROTRON XEOL

For the PS-based composite nanostructure containing more than one light emitting materials, how to identify the origin of the luminescence from each component is a very challenging problem. We utilized a technique known as synchrotron XEOL. XEOL employs a light source with widely tunable photon energies, enabling a site- and element-specific study of the origin of the luminescent components.[19,23] The element specificity comes about when the photon energy is tuned to a particular edge of an element of interest. The site specificity comes about when the excitation is tuned to a specific excitation channel that couples effectively with the chromophore of the luminescence. In Fig. 9, we measured the XEOL spectra of the CdS/PS composite excited with selected photon energies below and above the Si *K* edge and S *K* edge. For the purpose of comparison, the XEOL spectra of plain PS as well as that of a colloidal CdS nanoparticle [~2 nm quantum dots (QDs)] sample[22] are also shown. The plain PS shows a broad luminescence band centered around 700 nm. The luminescence maximum for the CdS QDs appears at ~540 nm. Both of these two spectra are similar to those recorded with ultraviolet excitation. Interestingly, the XEOL spectra of CdS/PS excited below and above Si *K* edge vary considerably. The luminescence spectrum excited below Si *K* edge displays a maximum at ~530 nm (green), which is more like the XEOL of CdS QDs, and the luminescence in orange-red region is suppressed significantly. In contrast, the XEOL excited above the Si *K* edge is predominated by a broadband centered around 700 nm (orange-red), similar to that of plain PS. A close inspection of spectrum c and d reveals that the Si *K* edge excitation turns on the PS luminescence but a weak luminescence feature centered around 530 nm still exists. These observations can be interpreted by considering the fraction of the photons absorbed by the composite below and above the Si *K* edge. When the incident photon was tuned from above the Si *K* edge to below the edge, the Si one absorption length (1/*e* attenuation) increases by more than tenfold (decrease in absorption coefficient). This means that below the Si *K* edge, a small fraction of the incidence photons are absorbed by Si atoms in the PS layer in comparison with the situation above the edge. Consequently, the broad orange-red XEOL band associated with nanosilicon was suppressed dramatically in spectrum c. However, the green luminescence band from the CdS deposits is now very visible in this spectrum. These observations indicate that both nano-CdS and PS contribute to the luminescence, although the luminescence from CdS is partially covered by the very broad and intense band from PS, as is seen in spectrum d.[25] When the excitation photon energies are tuned to higher energy, i.e., below (spectrum e) and above (spectrum f) S *K* edge (~2472 eV), both of the XEOL spectra become more intense. In these cases, the nano-CdS and PS both contribute since they can absorb enough photons at these excitation photon energies and the PS layer is significantly thicker (several micron) than the CdS overlayers (~100 nm).

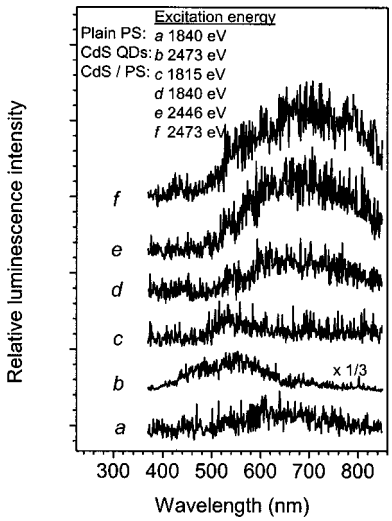

FIG. 9. XEOL spectra of (a) plain PS, (b) colloidal CdS QDs, (c)–(f) CdS/PS samples. The corresponding excitation photon energies are given in the figure.

VI. SUMMARY

Nanostructured CdS were successfully deposited on a PS substrate. These CdS deposits are uniformly distributed particles of ~100 nm, each consisting of many smaller nanocrystallites (~6 nm). The CdS nanostructure was observed by high-magnification SEM and confirmed by XRD studies. The structure and electronic properties of the nano-CdS were studied by XAFS measurements that confirmed the crystalline nature of the CdS nanostructure and revealed the presence of surface sulfate oxide in the aggregates. No significant deposition of CdS into the pore was observed under the present experimental conditions. Finally, the technique of synchrotron XEOL was demonstrated to be a powerful tool to identify the origin of the optical luminescence from the CdS deposits and the PS substrate.

ACKNOWLEDGMENTS

Research at UWO and CSRF is supported by NSERC and NRC (Canada). SRC is supported by the US NSF Grant

No. DMR-00-84402. The authors thank CSRF staff scientists K. H. Tan and Y. F. Hu for their assistance in the measurements at the CSRF–DCM beamline and the staff at SSW for the SEM and AFM measurements. P. Z. and P. S. K. gratefully appreciate an Ontario Graduate Scholarship and an Ontario Graduate Scholarship of Science and Technology, respectively, to support their graduate research.

[1] Nanoscale Materials Special Issue, edited by J. R. Heath, Acc. Chem. Res. **32**, 5 (1999).
[2] *Nanotechnology*, edited by G. Timp (AIP, New York, 1999).
[3] T. Ogino, H. Hibino, Y. Homma, Y. Kobayashi, K. Prabhakaran, K. Sumitomo, and H. Omi, Acc. Chem. Res. **32**, 447 (1999).
[4] *Properties of Porous Silicon*, edited by L. T. Canham (INSPEC, London, 1997).
[5] S. Fan, M. G. Chapline, N. R. Franklin, T. W. Tambler, A. M. Cassell, and H. Dai, Science **283**, 512 (1999).
[6] I. Coulthard, T.-T. Jiang, J. W. Lorimer, T. K. Sham, and X.-H. Feng, Langmuir **9**, 3441 (1993).
[7] T. K. Sham, I. Coulthard, J. W. Lorimer, A. Hiraya, and M. Watanabe, Chem. Mater. **6**, 2085 (1994).
[8] I. Coulthard, S. Degan, Y.-J. Zhu, and T. K. Sham, Can. J. Chem. **76**, 1707 (1998).
[9] I. Coulthard and T. K. Sham, Solid State Commun. **105**, 751 (1998).
[10] Y.-J. Zhu, I. Coulthard, and T. K. Sham, J. Synchrotron Radiat. **6**, 529 (1999).
[11] I. Coulthard, R. Sammynaiken, S. J. Naftel, P. Zhang, and T. K. Sham, Phys. Status Solidi A **182**, 157 (2000).
[12] P. Zhang, P. K. Kim, and T. K. Sham, J. Electron Spectrosc. Relat. Phenom. **119**, 229 (2001).
[13] M. Gros-Jean, R. Herino, and D. Linocot, J. Electrochem. Soc. **145**, 2448 (1998).
[14] A. S. Baranski, W. R. Fawcett, A. C. McDonald, and R. M. de Mobriga, J. Electrochem. Soc. **128**, 963 (1981).
[15] L. T. Canham, M. R. Houlton, W. Y. Leong, C. Pickering, and J. M. Keen, J. Appl. Phys. **70**, 422 (1991).
[16] Note: We also electrodeposited CdS on plain Si wafer under similar conditions. But no such CdS nanostructures were found in the SEM measurements. This observation is in contrast to a previous report of CdS on tin oxide using pulse electrodeposition in which ~5 nm CdS deposits were observed. For reference, see Y. Mastai, D. Gal, and G. Hodes, J. Electrochem. Soc. **147**, 1435 (2000).
[17] R. Jenkins and R. L. Snyder, *Introduction to X-Ray Powder Diffractometry* (Wiley, New York, 1996).
[18] D. S. Boyle, P. O'Brien, D. J. Otway, and O. Robbe, J. Mater. Chem. **9**, 725 (1999).
[19] *Chemical Application of Synchrotron Radiation*, edited by T. K. Sham (World Scientific, Singapore, 2001).
[20] D. Li, G. M. Bancroft, M. Kasrai, M. Fleet, X.-H. Feng, and K. Tan, Can. Mineral. **33**, 949 (1995).
[21] L. Troger, D. Arvanitis, H. Rabus, L. Wenzel, and K. Baberschke, Phys. Rev. B **41**, 7297 (1990).
[22] P. Zhang, S. J. Naftel, and T. K. Sham, J. Appl. Phys. **90**, 2755 (2001).
[23] T. K. Sham *et al.*, Nature (London) **363**, 331 (1993).
[24] Note: Cl^- species is probably absorbed from the starting material $CdCl_2$ in the solution during the deposition of CdS. However, this does not influence the similarity of the two EXAFS spectra in k space up to 8.3 $Å^{-1}$. A more detailed EXAFS study employing non-Cl^- starting material, $Cd(CH_3COO)_2$, is under way.
[25] Note: The UV-excited luminescence spectrum is similar to spectrum d.